An Equivalent Circuit Simulation of an AC Corona Discharge Air Ionizer − Frequency Dependence of Neutralization Performance −

M. Okano[1], T. Ikehata[1], and T. Terashige[2]
[1]Institute of Quantum Beam Science, Ibaraki University, Hitachi, Japan
[2]Teacher Education Unit, Hiroshima International University, Hiroshima, Japan

Abstract - AC corona discharge air ionizers have been used to neutralize the static electricity in inspection process for preventing faulty operations of electronic circuits and/or devices. The neutralization performance that is a neutralizing current density (J_W) and an electric field noise (E_W) depends on the operating conditions of air ionizers.

The equivalent circuit simulation method was proposed by using Simulation Program with Integrated Circuit Emphasis (SPICE) to find out the optimal operating condition without stopping production lines. In the simulation, the ion generation characteristic was simulated by a circuit composed of diodes and resistors. The transportation and accumulation of the ions were simulated by resistors and capacitors. The annihilation of ions based on recombination was simulated by capacitors and resistors.

In this study, we deal with the simulation for dependence on operating frequency of the neutralization performance of an AC corona discharge air ionizer. The simulated results were in good agreement with the experimental results in the frequency range from 2 to 25 Hz.

Keywords - Air ionizer, corona discharge, SPICE, simulation, neutralization performance, semiconductor manufacturing

I. INTRODUCTION

In manufacturing processes of electronic devices, static electricity could cause electrostatic induction that lead to electrostatic attraction ESA of unwanted particulate contaminants and/or electrostatic discharge ESD[1-3], which influence the yield reduction. Moreover, electrostatic induction and electrostatic discharge could cause electromagnetic interference EMI that leads to faulty operations in the inspection processes, which also reduces the manufacturing yield of those electronic devices[4,5].

The use of air ionizers is one of the effective solutions against these problems[6-10]. An air ionizer generates positive/negative ions to neutralize the undesired charges. An AC corona discharge air ionizer is most widely used among these air ionizers for manufacturing process of electronic devices[11-14].

However, the AC corona discharge air ionizer has negative side effects: In the air ionizer, high voltage (several kV) is applied to a needle shaped emitter to generate ions. The high voltage and/or generated ions themselves generates an electric field noise which could influence on the characteristics of the electronic devices such as the faulty operation and reduction of the manufacturing yield in the inspection process[2-4,15-18]. Consequently, it is required for air ionizers used in inspection processes that the electric field E_W is low enough. Also, high neutralizing current density J_W at the work area is desirable for rapid static neutralization[14].

The performance of the air ionizer depends on operating conditions such as a voltage applied to the emitter, an operating frequency, an air flow speed and a distance between the emitter and the work area. Therefore, the users of those air ionizers have to recognize the relationship between those operating conditions and the static neutralization performance so that they can use those air ionizers in optimal conditions.

However, it takes a long time to check the relationship and is required to stop the manufacturing line to decrease the productivity. Furthermore, the damage of the emitter and particle adhesion on the emitter tip change the ion generation characteristics of the air ionizer as time proceeds[19-22]. So we have to check periodically the conditions of air ionizers. During the checking the ion generation characteristics, the production lines have to be stopped, which reduces the productivity as well.

It may be very effective and convenient if the computer simulation can be applicable to estimate the relationship between the neutralization performance and the operating conditions by measuring only basic characteristic of an air ionizer with stopping a production line for a short time. Generally, a behavior of ions generated by an air ionizer is calculated with Finite Element Method (FEM)[23-24]. However, the usage of FEM simulation are not enough easy for beginners. Therefore, we try to build up a simulation system to estimate a neutralization performance by using the Simulation Program with Integrated Circuit Emphasis (SPICE)[25] which is familiar to electronics engineers.

In this study, we compare the results of simulation with experimental observations on the frequency dependence of the neutralizing current density J_W and the frequency dependence of the electric field E_W generated by the emitters and the ions.

Corresponding author: Makoto Okano
e-mail address: makotech1031@yahoo.co.jp
Submitted: May 26, 2019, Accepted: Oct. 20, 2019

II. EQUIVALENT CIRCUIT MODEL

The positive and negative ions are generated by an AC corona discharge air ionizer when the voltage applied to the emitter V_E exceeds the corona inception voltage V_{CS}. The ions are transported to the work area by the air flow, while being annihilated by recombination as shown in Fig. 1(a). The amount of the generated ion per unit time is equivalent to the emitter current.

We propose an equivalent circuit for the ion generation and the transportation of the air ionizer as shown in Fig. 1(b). In this figure, the top is the ion generation area. In this research, we surveyed an estimation of the neutralization performance, when the distance between the emitters and the work area D_{EW} was varied in the range of 0.3~0.7m because generally D_{WE} is around 0.5 m in inspection processes. The transportation area is divided into 7 layers which are numbered as N_L=1 (1st layer) at the bottom and N_L=7 (7th layer) at the top. The thickness of each layer is assumed to be 0.1m. Therefore, the distance between the emitter and the work area D_{EW} can be selected in the range of 0.1-0.7m.The right-hand side denotes of the equivalent circuit for the transportation area of positive ions while the left-hand side denotes the one of negative ions: The circuit current can flow, when the voltage across the diodes D_{PG}, D_{NG} exceed the threshold voltage V_T. The ion generation characteristics are simulated by the dynamic characteristics of diodes D_{PG}, D_{NG} and resistors R_{P1}-R_{P7}, R_{PG}, R_{N1}-R_{N7}, R_{NG}, where R_{PG} (R_{NG}) are the resistance of positive (negative) ion generation layer and R_{P1}-R_{P7} (R_{N1}-R_{N7}) are the resistance of each transportation layer for positive (negative) ions. In this circuit, the threshold voltage V_T of the diode corresponds to the corona inception voltage V_{CS} of the air ionizer. The ions accumulated in transportation layers as space charges are represented by the charges stored in capacitors C_{P1}-C_{P7}, C_{N1}-C_{N7}. The annihilation of ions due to recombination is represented by resistors R_{R1}-R_{R7} connecting adjacent positive and negative capacitors, C_{P1}-C_{P7}, C_{N1}-C_{N7}.

III. BASIC CHARACTERISTICS OF AIR IONIZER

In order to determine the circuit parameters of the equivalent circuit shown in Fig. 1(b), the basic characteristics of the corona discharge air ionizer, such as the ion generation characteristic and the electric field noise characteristic are examined.

A. Ion generation characteristic

We investigated the relationship between the emitter current and the emitter voltage because the amount of the ions generated by the air ionizer per unit time is equivalent to the emitter current. The measurements were performed in the mini-environment having a sidewall made by acrylic as shown in Fig.2. The work area is area of 1m×1m which is enough area to maintain the uniform air flow speed to a printed circuit board. It is confirmed that the ion density distribution and the air flow speed distribution are uniform at less than 0.3m in a domain from the center of the working area.

In this setup, the temperature and the relative humidity are 20°C and 40% respectively and an air flow with a speed of 0.3m/s was kept downwards.

In this setup, an air flow with a speed of 0.3m/s was kept downwards. A corona discharge air ionizer was put on the upper side of the work area. A metal plate of 500 × 500mm^2 which was insulated from the work area and was grounded through an ammeter was equipped for measuring the current at the work area. The amount of the positive ions and the negative ions was measured as the emitter current I_{EP}, I_{EN} with changing the emitter voltage V_E from 0 to +9.0kV and 0 to -9.0kV, respectively. Fig.3 shows the absolute value of I_{EP}, I_{EN} and I_{EA} as a function of the emitter voltage. The current I_{EA} means the average of the absolute value of I_{EP} and I_{EN}. In this figure, the corona inception voltage is found to be 3.0 kV. The typical operating voltage V_{E0} is defined as 2.5 times of the corona inception voltage V_{CS}, namely V_{E0} is defined as 7.5kV in this research. The current at V_{E0} is 2400nA, which is defined as the typical operating current I_0. It is to be noted that the I_{EA} - V_E curve shown in Fig. 3 can be modeled by an equivalent circuit consisting of a series connection of a diode and a resistor.

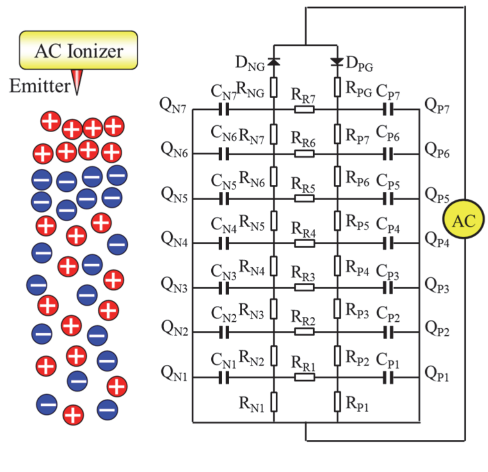

(a)Air ionizer (b) Equivalent circuit

Fig. 1. Schematic model of ion transportation and equivalent circuit model of AC corona discharge air ionizer.

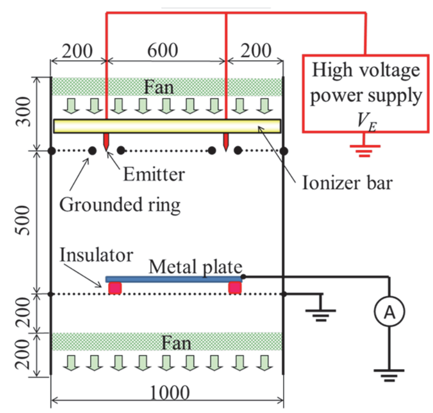

Fig. 2. Experimental setup using mini-environment

B Electric field noise characteristic

The electric field noise from emitters (E_{WE}) was measured using CPM[14] in the mini-environment as a function of the emitter voltage V_E. In order to avoid influence of the electric field caused by the generated ions, the measurement was carried out at an emitter voltage lower than the corona inception voltage. Then, square wave with voltage ranging from 0 to 6.0kV$_{PP}$ was applied to the emitter. Fig 4 shows E_{WE} as a function of V_E. From this figure, E_{WE} is found to be proportional to V_E.

IV. Definition of Circuit Parameters

In order to simulate the neutralization performance of the AC air ionizer by using the equivalent circuit, we need to determine the values of the following circuit parameters:

1) Resistors: R_{P1}-R_{P7}, R_{PG}, R_{N1}-R_{N7}, R_{NG}
2) Capacitors: C_{P1}-C_{P7}, C_{N1}-C_{N7},
3) Resistors: R_{R1}-R_{R7}.

We consider only the right-hand side of the equivalent circuit as shown in Fig 5, because it is bisymmetry.

A. Resistors for ion transportation

The current-voltage characteristics of diodes are associated with the relationship between the emitter current I_{EA} and the emitter voltage V_E. The resistances of R_{P1}-R_{P7}, R_{PG} are determined from the ion generation characteristics of the emitter. The static characteristic (I_{SS} - V_S) of the diode which was simulated on SPICE[25] is shown in Fig.6. We define the threshold voltage V_T, as the voltage where the tangent line at the typical operating current I_0=2400nA crosses the voltage axis: It is evaluated to be 1.42V in Fig.6. We further define the typical operating voltage V_{S0}=2.5V_T as the relation of V_{E0}=2.5V_{CS} in the actual air ionizer shown in Fig. 3. From the static characteristic in Fig. 6, V_{S0} is evaluated to be 3.55V and the diode voltage V_D for I_0 becomes 1.6V.

We consider that the I-V characteristics of the actual air ionizer and the SPICE diode should be similar if the same operating current of I_0= 2400nA flows at typical operating voltages, V_{E0} and V_{S0} though the voltage values are different. In the SPICE diode, it will be realized by connecting a resistor R_{P0} in series to the diode. The resistor R_{P0} has been divided into R_{P1}-R_{P7}, R_{PG} in the simulation model shown in Fig. 5. Thus, R_{P0} is derived as follows:

$$R_{P0} = \frac{V_{S0} - V_D}{I_0} . \cdots (1)$$

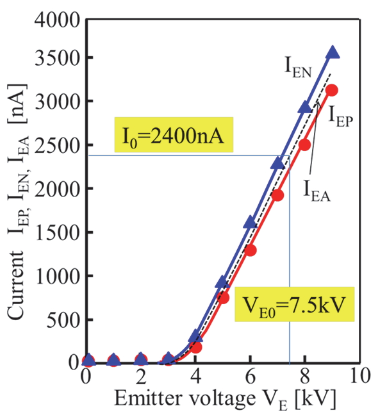

Fig. 3. Emitter current as a function of emitter voltage of a corona discharge air ionizer.

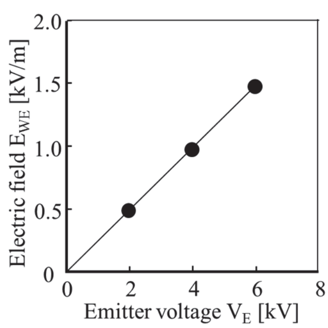

Fig. 4. Electric field from emitter at work area as a function of emitter voltage.

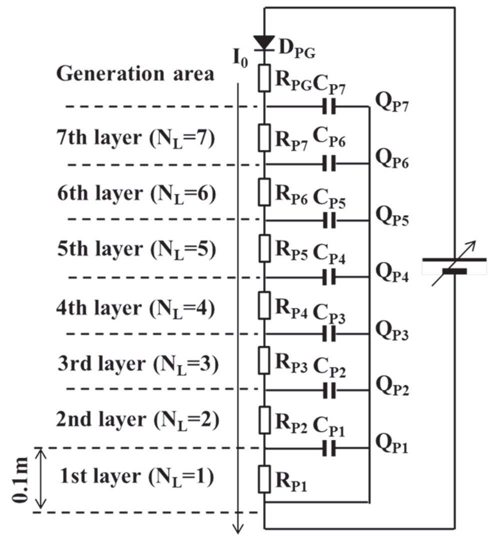

Fig. 5. Equivalent circuit model for positive ion of AC corona discharge air ionizer.

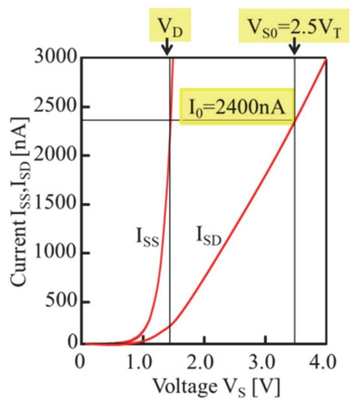

Fig. 6. Current - voltage characteristics of diode used in simulation. I_{SS}: static characteristic, I_{SD}: dynamic characteristic.

The resistance R_{P0} becomes 813kΩ from equation (1). Therefore, each resistance of the 8 resistors R_{P1}-R_{P7}, R_{PG} is 102kΩ if all of them have the same values.

The dynamic characteristic (I_{SD} - V_S) of the diode with resistance R_{P0} is shown in Fig.6. The simulated and measured dynamic characteristics are shown in Fig.7. In this figure, the voltage used for the simulation (V_S) is converted to the equivalent emitter voltage (V_{ES}) using

$$V_{ES} = \frac{V_{CS}}{V_T} V_S . \cdots (2)$$

In this figure, I_{SD} and I_{EA} are in good agreement around the typical operating voltage (V_E = 7.5kV).

B. Capacitors for space charge

When the ions are transported downwards by the air flow at a speed of U_A, the charge in each layer Q_L is expressed by the emitter current I_0 and the layer thickness T_L as

$$Q_L = \frac{I_0}{U_A} T_L . \quad \cdots (3)$$

Then the charge Q_L becomes 800nC, when I_0, U_A and T_L are 2400nA, 0.3m/s and 0.1m, respectively.

From the charge Q_L and the voltage across the capacitor, we can determine the capacitance. The voltage across the 1st layer V_{P1} is related to R_{P1} as

$$V_{P1} = I_0 R_{P1} . \cdots (4)$$

From R_{P1}=102kΩ and I_0=2400nA discussed above, V_{P1} is evaluated to be 0.245V. Then, the capacitance of the 1st layer C_{P1} is determined as 3.27 μF according to the following formula:

$$C_{P1} = \frac{Q_L}{V_{P1}} . \cdots (5)$$

The capacitance of C_{Pi} in Fig. 5 is inversely proportional to N_L because the charge Q_L in each capacitor C_{P1}-C_{P7} is constant and the voltages V_{P1}-V_{P7} applied to each capacitor C_{P1}-C_{P7} is proportional to N_L.

C. Resistors for ion recombination

The positive and negative ions generated by the air ionizers are annihilated due to the recombination in the transportation process.

Assuming that the generated ions are transported to the work area in t_F seconds, the ratio of the ion density at the work area (n_W) to that at the generation area (n_G) is approximated as[26]

$$\frac{n_W}{n_G} = \exp(-\frac{t_F}{\tau}) \cdots (6)$$

where τ is relaxation time of the ions. The ratio n_W/n_G is obtained by measuring the ratio of the current at work area I_W to that at generation area I_G.

The annihilation characteristics mentioned above are simulated. Each layer is composed of the resistors related to transportation area R_{Pi}, R_{Ni}, the resistor related to the recombination R_{Ri} and capacitors C_{Pi}, C_{Ni} as shown in Fig.8 (a). One side of each capacitor in each layer is grounded and the other side is connected to the power line. The equivalent circuit shown in Fig.8 (a) is simplified as shown in Fig.8 (b). Positive and negative charges accumulated in the capacitors C_{Pi}, C_{Ni} are annihilated through the resistor R_{Ri}. The current based on the recombination I_{Ri} is expressed as

$$I_{Ri} = I_{R0i} \exp(-\frac{t_F}{\tau}) \cdots (7)$$

where I_{R0i} is the current due to the recombination at the initial state. The relaxation time τ in equation (6), (7) is expressed by

$$\tau = \frac{C_{Pi} R_{Ri}}{2} \cdots (8)$$

therefore, the resistance of R_{Ri} is

$$R_{Ri} = \frac{2\tau}{C_{Pi}} . \cdots (9)$$

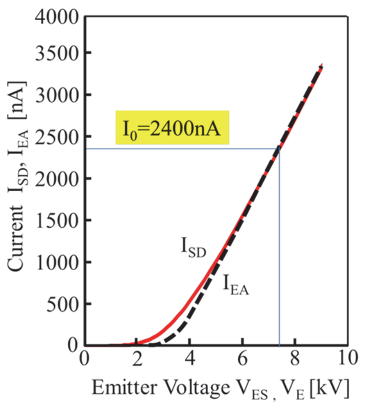

Fig. 7. Simulated (I_{SD},V_{ES}) and experimental(I_{EA},V_E) results on relationships between current and applied voltage.

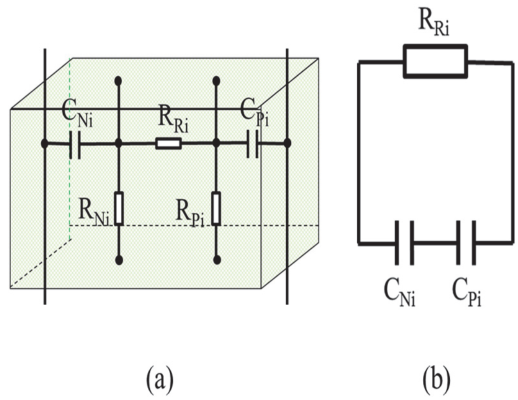

Fig. 8. Equivalent circuit of each layer.

It has been reported that a ratio I_W/I_G is 0.12 when the air ionizer is operated under the condition that the frequency f, the applied voltage V_E, the air flow speed U_A, the distance between emitters and the work area D_{EW} are 10Hz, 15kV$_{PP}$, 0.3m/s, 0.3m, respectively[27]. The ratio I_W/I_G is expressed as

$$\frac{I_W}{I_G} = \exp\left(-\frac{1.0}{\tau}\right) = 0.12 \cdots (10)$$

because the flight time of the ions is 1.0s under the operating condition mentioned above. Then, the relaxation time τ is obtained as 0.47s. The resistance of R_{R1}, that is resistance in the 1st layer (N_L=1), is obtained as 0.29MΩ by substituting 0.47s and 3.27μF for τ and C_{P1} in equation (9).

The resistance of R_{Ri} is proportional to N_L, because the relaxation time τ of the recombination in each layer is constant and is the product of R_{Ri} and C_{Pi} which is inversely proportional to N_L.

D. Equivalent circuit on SPICE

From above considerations, we finish building up the equivalent circuit for 10Hz on SPICE with putting the obtained parameters as shown in Fig.9.

The equivalent circuits corresponding to the other frequencies were designed to simulate the frequency dependence of the performance of the air ionizer. The resistors (RP1-RP7, RPG, RN1-RN7, RNG) and the capacitors (C P1-CP7, CN1-CN7) are independent of an operating frequency. The resistors (RR1-RR7) are determined by following the process shown in the chapter "*C. Resistors for ion recombination*".

V. SIMULATION FOR NEUTRALIZATION PERFORMANCE

The equivalent circuit shown in Fig.9 was set on SPICE. The frequency dependence of the neutralizing current density J_{SW} and the electric field E_{SW} at the work area were simulated under the following operating conditions:

1) Operating current I_0 = ±2400nA (square pulse),
2) Air flow speed U_A=0.3m/s,
3) Distance between the emitters and the work area D_{EW} = 0.5m,
4) Frequency range f = 2-25Hz.

The neutralizing current density J_{SW} was obtained from the current flowing through the resistor R_{P3}, because 3rd layer is the typical layer which is corresponding to 0.5m of a distance between the emitter and the work area D_{EW} in the mini-environment. The frequency dependence of the neutralizing current densities J_{SW} is shown in Fig. 10.

Electric field at the work area E_{SW} is composed of E_{WI} that is an electric field from the ions in the transportation area and E_{WE} that is an electric field from the emitter. The electric field from the emitter E_{WE} was extrapolated from the relationship shown in Fig.4, and was 3.0kV$_{PP}$/m.

On the other hand, E_{WI} was simulated by following procedure. First, voltages V_{Pi}, V_{Ni} applied to capacitors in each layer C_{Pi}, C_{Ni} were obtained. Then the positive and negative charges in each layer Q_{Pi}, Q_{Ni} were calculated by the relationships between the voltages V_{Pi}, V_{Ni} and capacitances of C_{Pi}, C_{Ni}, then the total charges in each layer Q_{Li} were obtained by the sum of the positive and negative charges for each layer. Finally, the downward electric field E_{DWi} generated by Q_{Li} was obtained, and also E_{WI} was obtained from following equation:

$$E_{WI} = \sum_{i=1}^{7} E_{DWi} . \cdots (11)$$

The waveform and the peak to peak value of the electric fields E_{SW} are shown in Fig. 11 and Fig. 12, respectively.

In order to find out the optimum operating frequency, we use the ratio of the neutralizing current density J_{SW} to the electric field E_{SW}[14], because a high current density

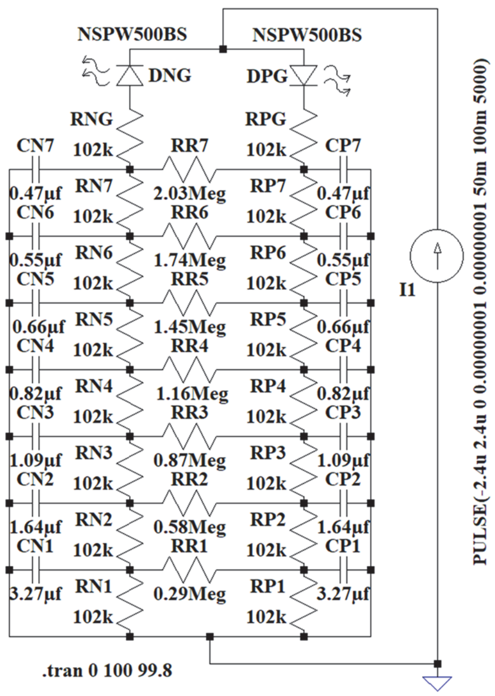

Fig. 9. Equivalent circuit with parameters for SPICE simulation

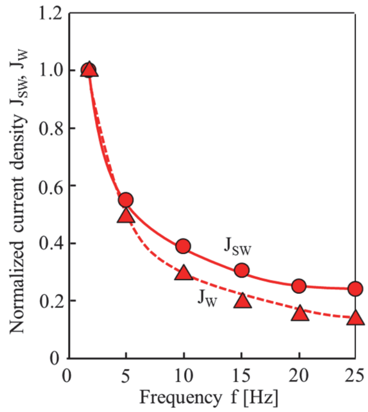

Fig. 10. Frequency dependence of normalized neutralizing current densities at work area, J_{SW}: simulated result, J_W: measured result.

and a low electric field are required for practical use in inspection process of electronic products. The ratio J_{SW}/E_{SW} is shown in Fig. 13. The ratio increases with increasing in the low frequency region and shows maximum value around 10Hz.

VI. Validity Evaluation of Simulation

The validity of the simulation is verified by comparing the simulated results with the experimental results. The frequency dependence of the performance has measured under the following conditions[28]:

1) Emitter voltage V_E =15kV$_{PP}$
2) Air flow speed U_A = 0.3m/s,
3) Distance between the emitters and the work area D_{EW} = 0.5m,

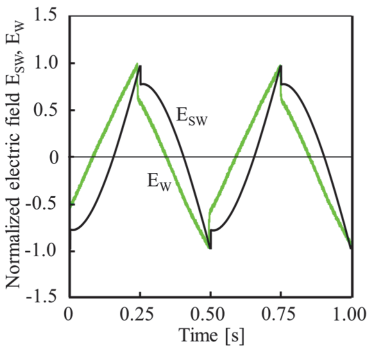

(a) 2Hz

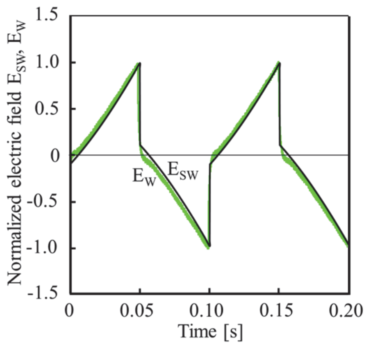

(b) 10Hz

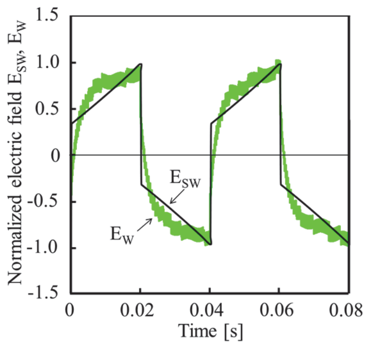

(c) 25Hz

Fig.11. Waveform of electric field at work area, E_{SW}: simulated result, E_W: measured result.

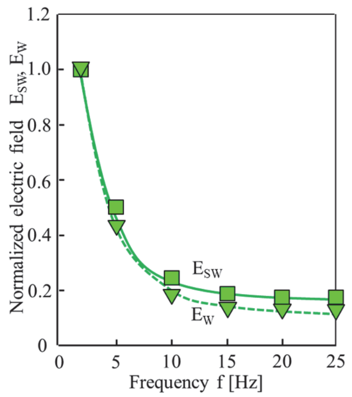

Fig. 12. Frequency dependence of normalized electric field, E_{SW}: simulated result, E_W: measured result.

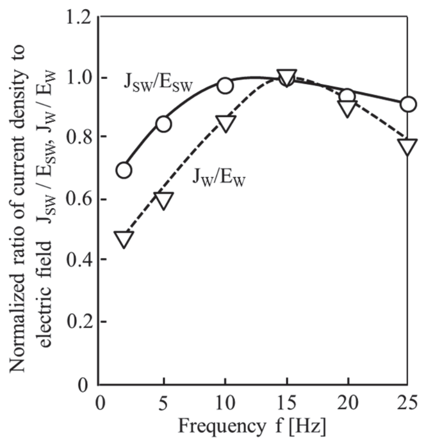

Fig. 13. Frequency dependence of normalized ratio of neutralizing current densities to electric field J_{SW}/E_{SW}: simulated result, J_W/E_W: measured result.

4) Operating frequency range f = 2-25Hz.

The neutralizing current densities J_{SW}, J_W, the electric fields E_{SW}, E_W and the ratios J_{SW}/E_{SW}, J_W/E_W are shown in Fig. 10, 11, 12, 13. In these figures, the simulated results J_{SW}, E_{SW}, J_{SW}/E_{SW} and the measured results J_W, E_W, J_W/E_W are normalized by each maximum value.

The frequency dependence of the neutralizing current densities (J_{SW}, J_W) is shown in Fig. 10. Both J_{SW} and J_W are decreased with increasing the frequency. The waveforms of the electric field are shown in Fig.11. In this figure, the air ionizer is operated with frequencies of 2, 10 and 25Hz. The simulated waveforms closely resemble the measured waveforms. The peak to peak value of the waveform was plotted in Fig. 12. The differences of the electric field between the simulated results and the measured results are less than 20%. The frequency dependences of the ratio J_{SW}/E_{SW}, J_W/E_W are shown in Fig. 13. The ratios show the peak value around 10Hz.

In these results, the simulated results J_{SW}, E_{SW}, J_{SW}/E_{SW} are in good agreement with the measured results J_W, E_W, J_W/E_W.

VII. CONCLUSION

An equivalent circuit simulation method was proposed for estimating a neutralization performance of AC corona discharge air ionizer. The validity of the simulation was verified by comparing the simulated results with the experimental results in the frequency range is of 2-25Hz which is the typical frequency range for conventional pulsed AC ionizers. The results are summarized as follows:

(1) Abrupt increase of the ion current around the corona inception voltage can be simulated by characteristics of diodes in the equivalent circuit.

(2) The ion current from the air ionizer to the work area can be simulated by current flowing through the resistors in the transportation area of the equivalent circuit.

(3) The recombination of the positive/negative ions in the transportation area can be simulated using the transient phenomena in CR net-work circuit.

(4) The simulated waveforms of the electric field closely resemble the observed waveforms.

(5) The simulated result of the frequency dependences of the ratio of the current to electric field is in good agreement with the experimental result.

From above results, the simulation using SPICE can be applicable to estimate the relationship between the neutralization performance and the operating conditions by measuring only basic characteristic of an air ionizer without stopping a production line.

In this paper, we investigated the frequency dependence of the neutralization performance as one of the operating conditions. We will investigate the validity of the simulation for the other operating conditions.

REFERENCES

[1] O. J. McAteer, “Electrostatic discharge control”, McGraw-Hill., U.S.A.,pp. 203-255, 1990.

[2] D. Krakauer, “ESD protection in a 3.3 V sub-micron silicided CMOS technology,” Journal of Electrostatics, vol. 31, Issues 2-3. pp. 111-129, 1993.

[3] S. U. Kim, “ESD induced gate oxide damage during wafer fabrication process,” Journal of Electrostatics, vol. 31, Issues 2-3. pp. 323-337, 1993.

[4] T. Terashige, D. Ohashi, and K. Okano, “Noise reduction of corona discharge air ionizer,” EOS/ESD Symposium, Charlotte, NC, U.S.A., pp. 243-247, 2002.

[5] S. Nagao, T. Terashige, and K. Okano, “Effect of space charge generated by air ionizer on noise in electric devices and/or electric circuit,” ECS Int’l Semiconductor Technology Conference, Shanghai, China, pp. 57-63, 2004.

[6] K. Asano, Y. Fukada, and T. Yasukawa, “Measurement of AC Ion current from a corona ionizer using a Faraday cage,” J. Electrostat., vol.66, Issues 2-3. pp. 275-282, 2008.

[7] H.Inaba, T.Ohmi, T.Yoshida, T.Okada, “Neutralization of Static Electricity by Soft X-Ray and Vacuum Ultraviolet-Ray Iraradiation,” IEICE Transactions on Electronics, vol.E79-C, No.3, pp.328-335, 1996.

[8] B. Pushpawela, “Efficiency of ionizers in removing airborne particles in indoor environments,” Journal of Electrostatics, vol.90, pp. 79-84, 2017.

[9] H. Inaba, S. Sakata, T. Yoshida, T. Okada, T. Ohmi, “Neutralization of wafer charging in nitrogen gas,” IEEE Trans. Semicond. Manuf., vol.5, pp. 359-367, 1992.

[10] D. Kim, “Characteristics of VUV ionizer in a vacuum chamber of flat panel displays,” Journal of Electrostatics, vol.90, pp. 54-60, 2017.

[11] T. Sugimoto, S. Kato, K. Furutachi, Y. Higashiyama, “DC Ionizer with opposed f-type corona electrodes for high-speed charge elimination,” IEEE trans. on Ind. App., vol.50, pp. 2207-2212, 2014.

[12] S. Sato, T. Ikehata, T. Terashige, and K. Okano, “Basic Characteristics of Self-control Discharge Air Ionizer,” IEEJ Trans. Electrical and Electronic Engineering, vol.11, No. S1, pp. S19-S23, 2016.

[13] D.Nemoto,W. He, T. Matsuo, N. Sato, T. Ikehata, K. Okano, “Static Elimination Performance of a Corona Ionizer Nitrogen-Based Electronegative Gases,” IEEE Trans. Ind. Appl., vol.52, No.5, pp. 4345-4350, 2016.

[14] M. Okano, “Effects of an electric field shield on the neutralizing characteristics of a corona discharge air ionizer,” IEEJ Trans. Electrical and Electronic Engineering, vol.12, pp. 147-148, 2017

[15] Mi Sook Kim, Seung Min Seen, and Seung Hee Lee, “The Static Electricity Resistant Liquid Crystal Display Driven by Fringe Electric Field,” Japanese Journal of Applied Physics, vol.51, 044201, 2012.

[16] M. Matsuo, “Silicon Interposer Technology for High-density Package,” Proc. 50th Electronic Components & Technology Conference, pp. 1456–1459, 2000.

[17] W. H. Lee, “MOS device structure development for ULSI: Low power/high speed operation,” Microelectronics Reliability, vol.37, pp. 1309–1314, 1997

[18] A. Steinman, “Static Control Issues for Disk Drive Production Using MR Heads,” Proceedings of 18 EOS/ESD Association Symposium, pp. 22–27, 1996.

[19] K. D. Murray, V. P. Gross and P. C. D. Hobbs: “Clean Corona Ionization,” 1990 EOS/ESD Symposium Proceedings, pp. 36-40 1990

[20] K. Okano and A. Posadas: “Particle Generation of Ceramic Emitters for Cleanroom Air Ionizers,” 1997 EOS/ESD Symposium Proceedings, pp. 287-291 1997

[21] C. G. Noll and P. A. Lawless: “Comparison of Germanium and Silicon Needles as Emitter Electrodes for Air Ionizers,” 1997 EOS/ESD Symposium Proceedings, pp. 195-204 1997

[22] H. Imazono, T. Terashige, and K. Okano, “The Double Jet Ionizer for ULSI Manufacturing Process,” IEEE Trans. Semiconductor Manufacturing, vol. 15, No.2, pp. 189-193, 2002.

[23] K. Adamiak, P. Atten, “Simulation of corona discharge in point–plane configuration,” Journal of Electrostatics, vol. 61, pp. 85-98, (2004)

[24] H. Ziedan, J. Tlustý, A. Mizuno, A. Sayed1, A. Ahmed1, and R. Procházka, “Finite Element Solution of Corona I-V Characteristics in ESP's with Multi Discharge Wires,” International Journal of Plasma Environmental Science & Technology, Vol.5, PP. 68-79 (2011)

[25] Amit Kumar Singh, Rohit Singh “Electronics Circuit Spice Simulations With LTspice: A Schematic Based Approach”, CreateSpace Independent Publishing Platform, 2015.

[26] S. Nakae, “Properties of Atmospheric Ion and Measuring Technics,” Earozoru_kenkyu, vol. 2, No. 2, pp. 111-116, 1987

[27] Y. Hirata, and K. Okano, “Transportation Efficiency of Ion Generated by AC Corona Discharge Air Ionizer,” J. Inst. Electrostatics Japan, vol. 38, No. 3, pp. 135-138, 2014

[28] M. Okano, T. Ikehata, T. Terashige, “Effects of Operating Frequency on Electric Field and Neutralizing Current Density of a Corona Discharge Air Ionizer,” International Journal of Plasma Environmental Science & Technology, vol. 12, No. 2, pp.120-124, 2019